Journal of Microscopy, Vol. 226, Pt 2 May 2007, pp. 175–181
Received 13 September 2006; accepted 11 February 2007

High-resolution compact X-ray microscopy

P. A. C. TAKMAN, H. STOLLBERG, G. A. JOHANSSON†,
A. HOLMBERG, M. LINDBLOM & H. M. HERTZ
Biomedical and X-Ray Physics, Royal Institute of Technology/Albanova, SE-106 91 Stockholm, Sweden

Key words. Compact, laser plasma, liquid-jet, soft x-ray microscopy, water window, zone plate optics.

Summary

We demonstrate compact full-field soft X-ray transmission microscopy with sub 60-nm resolution operating at $\lambda = 2.48$ nm. The microscope is based on a 100-Hz regenerative liquid-nitrogen-jet laser-plasma source in combination with a condenser zone plate and a micro-zone plate objective for high-resolution imaging onto a 2048 × 2048 pixel CCD detector. The sample holder is mounted in a helium atmosphere and allows imaging of both dry and wet specimens. The microscope design enables fast sample switching and the sample can be pre-aligned using a visible-light microscope. High-quality images can be acquired with exposure times of less than 5 min. We demonstrate the performance of the microscope using both dry and wet samples.

Introduction

Soft X-ray microscopy in the water window (λ = 2.34–4.37 nm) provides a unique set of high-resolution imaging capabilities that complement visible light and electron microscopy (Schmahl *et al.*, 1980; Kirz *et al.*, 1995). Organic materials show strong absorption in this region, whereas water is relatively non-absorbing. This intrinsic contrast mechanism enable imaging of unstained carbon-containing materials, such as biological specimens or polymers, with thicknesses up to ∼10 μm in an aqueous environment. Most present soft X-ray microscopes are based on high-brightness synchrotron-radiation sources (Meyer-Ilse *et al.*, 1998; Guttmann *et al.*, 2003). Typically they operate at λ = 2.4 nm, close to the oxygen K-absorption edge, thereby minimizing oxygen absorption. This enables imaging of both hydrated and dry samples with short exposure times. Nevertheless, the limited accessibility to synchrotron-based instruments reduces the impact of X-ray microscopy as an important tool for user-motivated research. We recently demonstrated a compact X-ray microscope operating in the water window at λ = 3.37 nm (Berglund *et al.*, 2000; Johansson *et al.*, 2002). However, imaging of thicker (∼10 μm) objects, for example, mammalian cells, requires operation in the lower wavelength range of the water window where the transmission is higher. In this paper we present a high-resolution compact soft X-ray full-field transmission microscope operating at λ = 2.48 nm using a liquid-nitrogen laser-plasma source.

High-resolution transmission X-ray microscopy was first developed by Schmahl *et al.* at the university of Göttingen in Germany (Niemann *et al.*, 1976; Schmahl *et al.*, 1993). A typical arrangement includes an X-ray source that illuminates the sample by means of a condenser. A micro-zone plate acts as a high-resolution objective. The magnified image is read out from a thinned back-illuminated CCD detector. The theoretical resolution in an X-ray microscope is limited by the outermost zone width of the zone plate (Attwood, 1999). Zone plates with zone widths down to 15 nm were recently demonstrated by Chao *et al.* (2005). X-ray microscopy can also be operated in scanning mode, something which was first demonstrated by Kirz *et al.* at Stony Brook (Rarback *et al.*, 1980; Jacobsen *et al.*, 1991).

Previous work on compact transmission X-ray microscopy in the water window has been based on laboratory-scale laser-plasma or pinch-plasma sources. A carbon-tape-target laser plasma was combined with an elliptical condenser mirror and a zone plate to perform λ = 3.37 nm imaging of dry test objects (Nakayama *et al.*, 1994; Aritome *et al.*, 2000). The magnification was 500× and periods down to 180 nm were resolved. The debris emission from and the non-regenerative character of the carbon-tape target resulted in a system with limited operability. Rudolph *et al.* (1994) combined a low-repetition-rate pinch-plasma source with an elliptical condenser mirror and zone plate optics for λ = 2.48 nm, demonstrating dry and wet imaging. The low repetition rate and the instability of the source made operation of the system difficult; still 100–150 nm features were detectable for dry objects with low signal-to-noise ratio.

Correspondence to: P. A. C. Takman. e-mail: per.takman@biox.kth.se
†Present address: Lawrence Berkeley National Lab, Advanced Light Source, 1 Cyclotron Road MS 6R2100, Berkeley, CA 94720-8226, U.S.A.

This microscope did not isolate the $\lambda = 2.48$ nm line from the $\lambda = 2.49$ nm line resulting in a large effective line width which caused chromatic aberrations in the zone-plate image, thereby limiting the extendability towards high-resolution X-ray microscopy. Berglund *et al.* (2000) demonstrated a $\lambda = 3.37$ nm microscope employing a normal-incidence spherical multilayer condenser mirror and zone plate optics with a resolution of ~100 nm. This microscope used a minimum-debris regenerative liquid-jet laser-plasma source (Rymell & Hertz, 1995). A different approach was recently demonstrated by Hoshino & Aoki (2006), where a broadband solid-tantalum-target laser-plasma source in combination with Wolter-type grazing-incidence mirrors used both as condenser and objective resulted in an estimated resolution ~100 nm. Kyong *et al.* (2006) combined an elliptical condenser mirror and zone plate optics for $\lambda = 2.88$ nm microscopy, claiming 50 nm resolution. Scanning microscopy with a laser-plasma source operating at 3.37 nm using a Mylar® target (DuPont Teijin Films, Hopewell, VA, USA) was demonstrated by Michette *et al.* (2003), and was capable of resolving structures with a period ~400 nm.

In the present paper we demonstrate a compact full-field soft X-ray transmission microscope with sub-60-nm resolution operating at a wavelength of $\lambda = 2.48$ nm. The shorter wavelength enables studies of hydrated samples up to ~10 μm thick. With the sample holder mounted in a helium atmosphere the microscope allows imaging of dry and wet specimens. The design permits fast sample switching, and a visible-light microscope is used for pre-alignment of the sample. High-quality images can be acquired with exposure times of less than 5 min. We demonstrate the performance of the microscope using both dry and wet samples.

Experimental arrangement

The experimental arrangement for the compact X-ray microscope is shown in Fig. 1. The arrangement includes a regenerative liquid-nitrogen-jet laser-plasma source, a condenser zone plate, a helium-filled sample environment, a micro-zone plate objective for high-resolution imaging, and a back-illuminated soft X-ray-sensitive CCD detector.

Liquid-jet laser-produced plasmas (Rymell & Hertz, 1993; Malmqvist *et al.*, 1996) are attractive, compact, high-brightness sources for soft X-ray radiation. These sources are spatially well defined, regenerative and allow high-repetition-rate operation with minimum debris emission (Rymell & Hertz, 1995). Hydrogen-like nitrogen ions emit strongly at $\lambda = 2.48$ nm making nitrogen an attractive laser-plasma target for compact soft X-ray microscopy in the lower range of the water-window wavelength region (Jansson *et al.*, 2005).

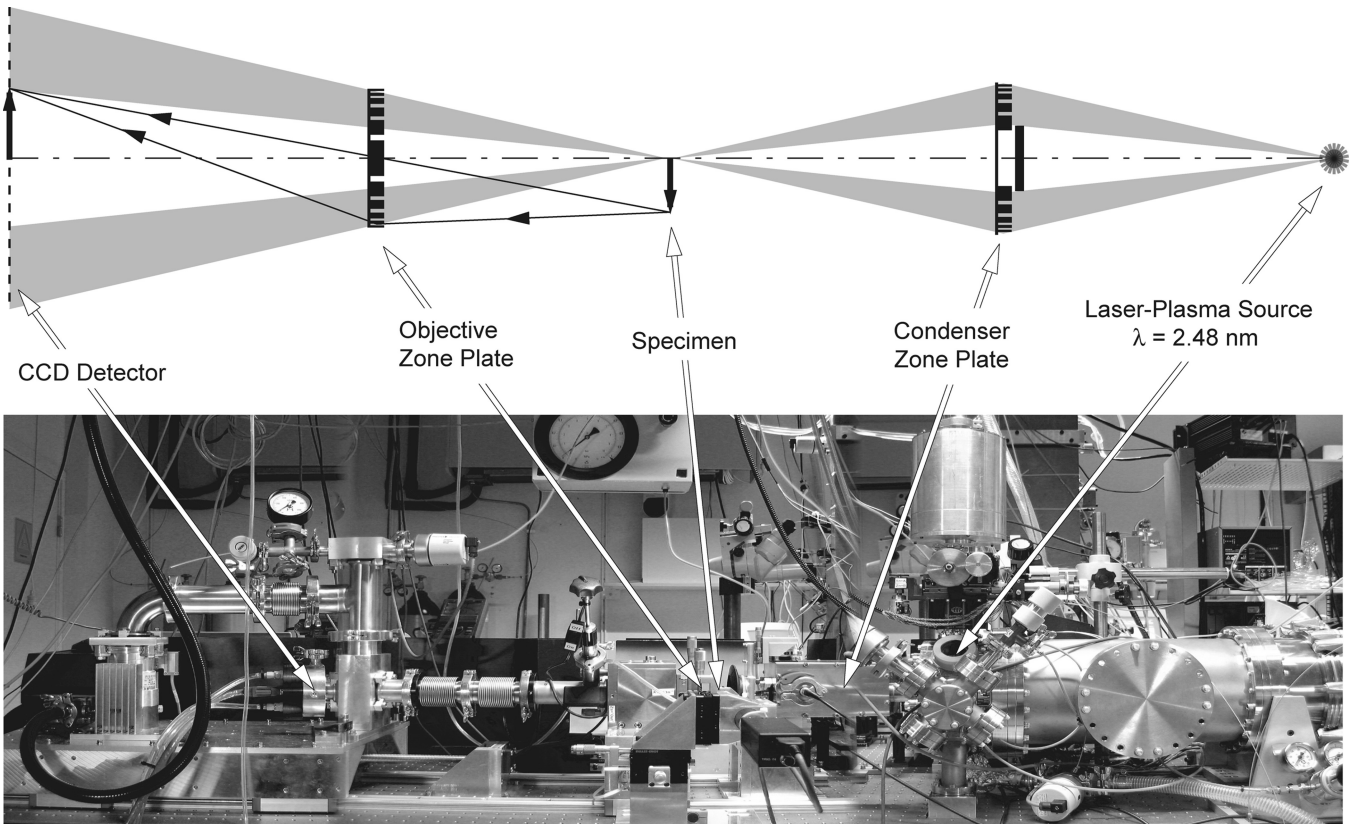

Fig. 1. Compact soft X-ray microscope arrangement.

Furthermore, the nitrogen source benefits from being relatively inert, thereby minimizing deposition on and damage to the sensitive X-ray optics due to debris. The liquid-nitrogen target delivery system employs a cryogenically cooled fused silica capillary nozzle with a 15–20 μm diameter orifice. The plasma is generated by a pulsed (100 Hz, ~3 ns), frequency-doubled Nd : YAG laser (Coherent Infinity 40–100) (Coherent Inc., Santa Clara, CA, USA). The beam is focused onto to the continuous part of the jet using a ~150-mm focal length lens. Pulse energies up to ~200 mJ, corresponding to focal intensities of $\sim 4 \times 10^{13}$ W/cm^2, can be achieved at the liquid-nitrogen jet target. The average X-ray flux is $\sim 1.0 \times 10^{12}$ photons/(pulse $\times$ sr $\times$ line) and the source size is ~20 μm full width at half maximum (Jansson *et al.*, 2005).

The condenser is a nickel zone plate in combination with a central stop (Rehbein *et al.*, 2004). Even though normal-incidence multilayer condenser mirrors are available at $\lambda = 3.37$ nm (Stollberg *et al.*, 2006) no mirrors have shown the required reflectivity and the necessary uniformity on sufficiently large substrates for $\lambda = 2.48$ nm. The condenser zone plate has a diameter of 4.53 mm and an outermost zone width of 49 nm. The focal length in the first diffraction order is 90 mm at $\lambda = 2.48$ nm. The measured absolute condenser zone plate efficiency is 7.6% at $\lambda = 2.48$ nm. The specimen is illuminated using critical illumination via 1:1 imaging of the source onto the object plane with a plasma-to-condenser distance of 180 mm. The numerical aperture of the illumination is 0.013. The condenser zone plate in combination with the central stop and a pinhole in front of the sample plane acts as a soft X-ray monochromator, selecting the $\lambda = 2.48$ nm emission line from the plasma. Furthermore, a 300-nm-thick free-standing chromium filter blocks scattered and direct visible light from the condenser.

The specimen is placed on a 100-nm-thick silicon nitride membrane in a sample holder that is held in place by a magnetic kinematic mount. There is also a wet specimen chamber option where the specimen is clamped in between two silicon nitride membranes. The sample holder is mounted in a helium atmosphere separated from the source-system vacuum by a silicon nitride membrane and from the CCD-system vacuum by the objective zone plate membrane. The design enables fast sample switching. Furthermore, a visible-light microscope with 20× magnification is used for accurate pre-alignment of the sample in situ.

High-resolution imaging is performed with nickel phase zone plates fabricated utilizing a tri-level nanostructuring process (Holmberg *et al.*, 2004). The patterns are generated by e-beam lithography and transferred by reactive ion etching and nickel electroplating. Table 1 gives the important parameters for the three objective zone plates that have been used to characterize the microscope. The measured first-order efficiency for the 25 nm zone plate is 8.9% at $\lambda = 2.48$ nm (Bertilson *et al.*, 2006). The mismatch in numerical aperture between the condenser and the objectives means that the microscope is operating with partially coherent illumination.

Table 1. Optical parameters for the objective zone plates used in the microscope.

Focal length @ $\lambda = 2.48$ nm [μm]	Outermost zone width [nm]	Number of zones	Diameter [μm]	Numerical aperture
546	25	550	54.5	0.050
682	30	500	58	0.043
1500	50	380	75	0.025

The image is detected by a cooled, thinned, back-illuminated 2048 × 2048 pixel CCD array (Princeton Instruments, Inc., Trenton, NJ, USA) with 13 × 13 μm^2 pixels and a quantum efficiency of ~0.65. By adjusting the distance between the detector and the objective zone plate, the magnification can be varied.

Results

The performance of the microscope was determined by imaging various test structures made of nickel. The test structures were fabricated using the same process as for the zone plates (Holmberg *et al.*, 2004). Figure 2 shows an image of a Siemens star recorded with a pixel element size of 24 × 24 nm^2 using 2 min exposure time. Siemens stars are useful for testing the imaging performance over the full field of view (FOV). As seen in the image the illumination is uniform over the full ~10 μm FOV. The insert in Fig. 2 shows the central part of the Siemens

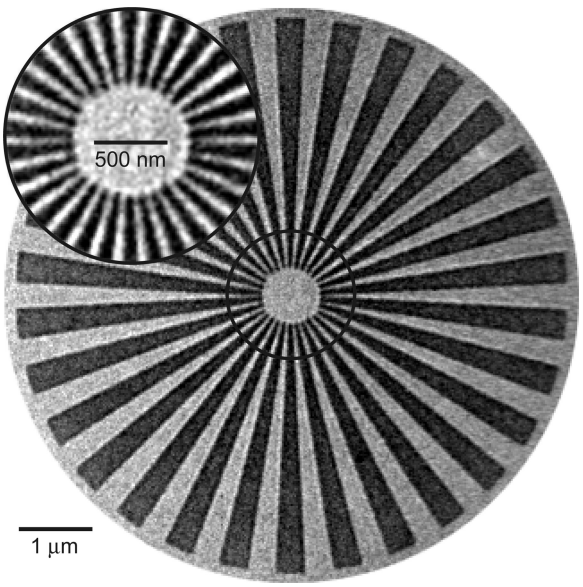

Fig. 2. Image of Siemens star recorded with a pixel element size of 24 × 24 nm^2 using 2 min exposure time. The insert shows the central part of the Siemens star.

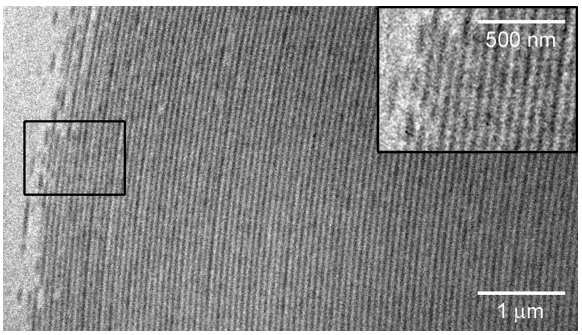

Fig. 3. Image of zone plate recorded with a pixel element size of 6.6 × 6.6 nm^2 using 5 min exposure time. The insert shows an enlargement of the squared region with 30 nm lines and spaces.

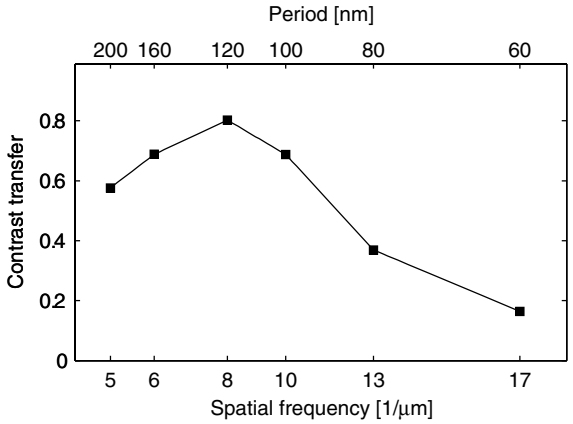

Fig. 4. Contrast transfer for gratings with periods from 200 nm to 60 nm.

star. Structures with a period of ∼80 nm are clearly resolved in all directions, with observable resolution limited by the test structure. The slight difference in resolution in different directions is due to astigmatism in the objective zone plate and possibly also a small amount of thermal drift during exposure.

The resolution of the microscope was determined by imaging a zone plate with 30 nm outermost zones using the 25 nm zone plate of Table 1. Figure 3 shows an image of the outermost part of the zone plate, recorded with a pixel element size of 6.6 × 6.6 nm^2 using 5 min exposure time. The insert shows an enlargement of the squared region. The 30 nm lines are imaged with good contrast.

In order to further characterize the optical performance of the microscope, gratings with periods from 200 nm to 60 nm have been imaged. Figure 4 shows the contrast transfer, defined as the image contrast divided by the object contrast, as a function of spatial frequency. The object contrast was calculated from the theoretical transmission of nickel. Figure 4 indicates that the microscope can perform imaging with sub 60-nm resolution. The details concerning the behaviour of contrast transfer in a partially coherent microscope has been investigated by von Hofsten (2006).

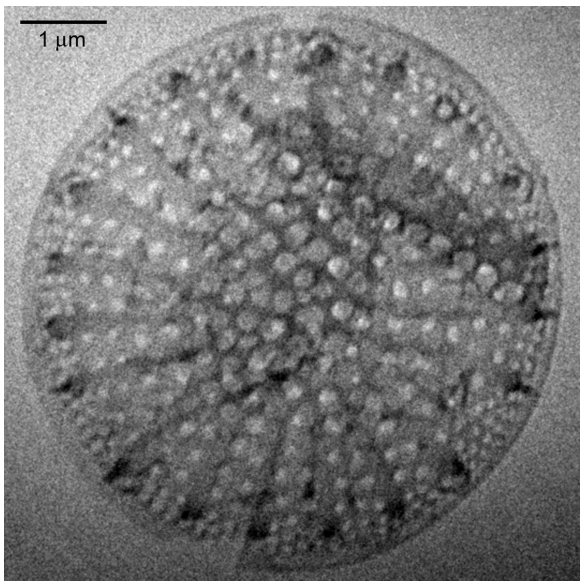

Fig. 5. Image of a diatom recorded with a pixel element size of 13 × 13 nm^2 using 5 min exposure time.

In addition to high resolution and contrast, high-quality imaging over the full object-plane FOV requires illumination with a good uniformity, which can be defined as $U = (I_{max} - I_{min})/(I_{max} + I_{min})$, where I is the image intensity. The hollow cone angle of the illumination arrangement in combination with the focal length of the micro-zone plate objective determines the FOV of the microscope. For the micro-zone plates used (*cf.* Table 1) the FOV varies from 10 to 26 μm. The illumination is nearly uniform over the full ∼10 μm FOV ($U = 0.10$). Using a larger FOV results in a less uniform illumination.

To demonstrate the applicability of the compact X-ray microscope for user-motivated research, both dehydrated and hydrated biological specimens were imaged. Figure 5 shows a diatom imaged with a pixel element size of 13 × 13 nm^2 using 5 min exposure time. Diatoms are eukaryotic algae with cell walls made of silicate, which show structures sized from several micrometers down to a few nanometres.

Figure 6 shows an image of a dehydrated COS-7 cell recorded with a pixel element size of 36 × 36 nm^2 using 5 min exposure time. We note the much higher transmission in the thick central part of the cell with the present $\lambda = 2.48$ nm microscope compared to the $\lambda = 3.37$ nm microscope (Hertz *et al.*, 2000). The employed adherent COS-7 cells, derived from foetal monkey kidney, were cultured in Dulbecco's modified eagles medium (*Sigma-Aldrich*) containing 10% foetal bovine serum (*Invitrogen*), 1% penicillin streptomycin (*Sigma-Aldrich*), and 1% L-glutamine (*Sigma-Aldrich*). A droplet (∼30–40 μL) of the medium with about 2 × 10^4 cells is placed on a silicon nitride membrane. The cells are then incubated for about 48 h at 37°C in 5% CO_2 atmosphere, while the medium is exchanged

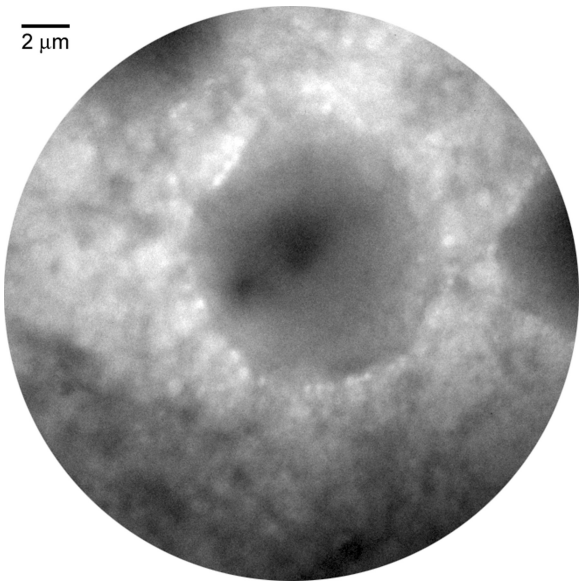

Fig. 6. Image of a dehydrated COS-7 cell recorded with a pixel element size of 36×36 nm^2 using 5 min exposure time.

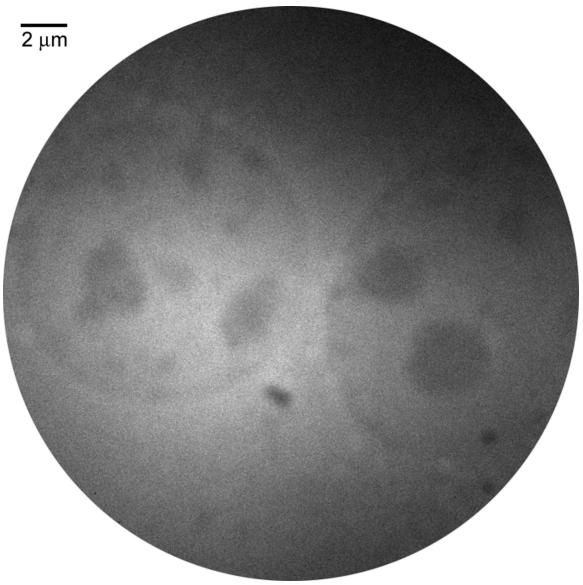

Fig. 7. Image of two COS-7 cells in an aqueous environment recorded with a pixel element size of 36×36 nm^2 using 5 min exposure time.

after 24 h. For preparation of the dry samples the medium is removed by careful rinse-off of the medium with PBS (*Sigma-Aldrich*). Dehydration of the cells is done by a series of ethanol-water washes.

When imaging wet specimens, most of the medium is removed so that only a thin layer of liquid is present on the silicon nitride membrane when the second membrane is put on top of the first one. Residual liquid is thereafter carefully removed. The achieved thickness of the liquid layer in between the silicon nitride membranes is below 10 μm. Figure 7 shows an image of two COS-7 cells in an aqueous environment recorded with a pixel element size of 36×36 nm^2 using 5 min exposure time. Both cell images were recorded using the 50 nm zone plate for increased FOV. Figures 6 and 7 appear to have moderate contrast. This is due to the non-uniform illumination profile obtained when using a large FOV, which makes contrast adjustment over the full image difficult without saturation of bright areas.

Discussion

We have demonstrated a compact full-field soft X-ray transmission microscope with sub-60-nm resolution operating at 2.48 nm wavelength, thereby enabling studies of samples with thicknesses up to ~10 μm. Images of dry samples using a pixel element size of 6.6×6.6 nm^2 and ~300 photons/pixel are acquired during a 5-min exposure. The quality of the images, for dry samples, are approaching those recorded using a synchrotron light source. Still there is room for improvements. Of special importance for the practical usefulness of the microscope are reduced exposure times. Currently the illumination of the sample is $\sim 10^5$ photons/($s \times \mu m^2$). Typically 10^7 to 10^8 photons/μm^2 are required for high-quality imaging, depending on the sample. Fortunately, the laser-plasma target delivery system allows operation at much higher repetition rates (Vogt *et al.*, 2001) than the present 100 Hz. A new kHz laser with similar pulse energy as the present laser will increase the average X-ray flux by nearly an order of magnitude. Further reduction in exposure time will be achieved with a new generation of condenser zone plates. By improving the overall pattern quality and increasing the total diameter of the zone plate we expect to reduce the exposure time by another factor of 3. Together these two improvements would result in exposure times on the order of 3–30 s, which is similar to synchrotron-based microscopes. It would also allow increased contrast via Zernike phase contrast, which requires higher photon flux, while maintaining reasonable exposure times. On a longer time scale, multilayer condenser mirrors also at this wavelength are feasible (Gullikson *et al.*, 2006). This would further reduce exposure times and also increase the resolution by improving the numerical aperture match between the condenser and the objective (Stollberg *et al.*, 2006).

In addition to the exposure time, application-oriented research requires simple and efficient sample handling and alignment. The present sample holder is mounted in a helium atmosphere and has the ability to image both dry and wet specimens. The design enables fast sample switching and the sample can be pre-aligned using a visible-light microscope. Due to the modular design of the sample compartment, the microscope can easily be adjusted to new applications. Of special future interest to cell biology is a sample module allowing cryogenic fixation of the sample since it reduces

radiation damage. Such a module would also enable X-ray tomography for 3D imaging (Larabell & Le Gros, 2004). Finally, we note that the microscope can be used for high-resolution imaging with chemical contrast in addition to the natural contrast, employing colloidal gold markers. Stollberg *et al.* (2007), recently demonstrated an image-analysis algorithm for the size-selective localization of single colloidal-gold particles in cell like structures. Gold particles down to a size of 50 nm could clearly be identified and localized by this algorithm.

Acknowledgements

The authors gratefully acknowledge S. Rehbein for his early work on the zone plate condenser and U. Vogt for insightful discussions concerning imaging using partially coherent illumination. We also thank R. Helg and K. Hammarström in the mechanical workshop for the work done on the design and building of the microscope. This work has been supported by the Swedish Science Research Council and the Göran Gustafsson Foundation.

References

Aritome, H., Fujii, M., Fujita, G. & Shinohara, K. (2000) An imaging zone plate X-ray microscope using a laser plasma source. *AIP Conf. Proc. (USA)* (ed. by W. Meyer-Ilse, T. Warwick & D. Attwood), pp. 401–404, AIP, Berkeley, California.

Attwood, D.T. (1999) *Soft X-Rays and Extreme Ultraviolet Radiation*. Cambridge University Press, Cambridge.

Berglund, M., Rymell, L., Peuker, M., Wilhein, T. & Hertz, H.M. (2000) Compact water-window transmission X-ray microscopy. *J. Microsc.* **197**, 268–273.

Bertilson, M., Takman, P.A.C., Vogt, U., Holmberg, A. & Hertz, H.M. (2006) Laboratory arrangement for soft x-ray zone-plate efficiency measurements. *Review of Scientific Instruments*. **78**, 026103-1-3.

Chao, W., Harteneck, B.D., Liddle, J.A., Anderson, E.H. & Attwood, D.T. (2005) Soft X-ray microscopy at a spatial resolution better than 15 nm. *Nature*, **435**, 1210–1213.

Gullikson, E.M., Salmassi, F., Aquila, A.L. & Dollar, F. (2006) Progress in short period multilayer coatings for water window applications. *The 8th International Conference on The Physics of X-Ray Multilayers Structures*, March 2006, Sapporo, Japan, abstract S8 O4.

Guttmann, P., Niemann, B., Rehbein, S., Knochel, C., Rudolph, D. & Schmahl, G. (2003) The transmission X-ray microscope at BESSY II. *Journal De Physique. IV : JP* (ed. by J. Susini, D. Joyeux & F. Polack), pp. 85–90, EDP Sciences, Grenoble, France.

Hertz, H.M., Berglund, M., Johansson, G.A., Peuker, M., Wilhein, T. & Brismar, H. (2000) Compact water-window X-ray microscopy with a droplet laser-plasma source. *AIP Conf. Proc. (USA)* (ed. by W. Meyer-Ilse, T. Warwick & D. Attwood), pp. 721–725, AIP, Berkeley, California.

Holmberg, A., Rehbein, S. & Hertz, H.M. (2004) Nano-fabrication of condenser and micro-zone plates for compact X-ray microscopy. *Microelectron. Eng.* **73–74**, 639–643.

Hoshino, M. & Aoki, S. (2006) Laser plasma soft x-ray microscope with Wolter mirrors for observation of biological specimens in air. *Japan J. Appl. Phys.* **45**, 989–994.

Jacobsen, C., Williams, S., Anderson, E., Browne, M.T., Buckley, C.J., Kern, D., Kirz, J., Rivers, M. & Zhang, X. (1991) Diffraction-Limited Imaging in A Scanning-Transmission X-Ray Microscope. *Opt. Commun.* **86**, 351–364.

Jansson, P.A.C., Vogt, U. & Hertz, H.M. (2005) Liquid-nitrogen-jet laser-plasma source for compact soft x-ray microscopy. *Rev. Sci. Instrum.* **76**, 43503–1-5.

Johansson, G.A., Holmberg, A., Hertz, H.M. & Berglund, M. (2002) Design and performance of a laser-plasma-based compact soft X-ray microscope. *Rev. Sci. Instrum.* **73**, 1193–1197.

Kirz, J., Jacobsen, C. & Howells, M. (1995) Soft-X-Ray Microscopes and Their Biological Applications. *Qtr. Rev. Biophys.* **28**, 33–130.

Kyong, W.K., Youngman, K., Ki-Yong, N., Jong-Hyeok, L., Kyu-Gyum, K., Kwon, S.C., Byoung, H.K., Dong, E.K., JinGon, K., Byoung, N.A., Hyun, J.S., Seungyu, R., Ki-Ho, K., Jin, S.C., Dae, G.G., Dong, W.K., Sung, H.K., Jin, Y.M., Kyu-Sil, C., Seong, E.Y., Eun, A., Yoshiharu, N. & Kwon-Ha, Y. (2006) Compact soft x-ray transmission microscopy with sub-50 nm spatial resolution. *Phys. Med. Biol.* **51**, 99–107.

Larabell, C.A. & Le Gros, M.A. (2004) X-ray tomography generates 3-D reconstructions of the yeast, Saccharomyces cerevisiae, at 60-nm resolution. *Mol. Biol. Cell* **15**, 957–962.

Malmqvist, L., Rymell, L., Berglund, M. & Hertz, H.M. (1996) Liquid-jet target for laser-plasma soft X-ray generation. *Rev. Sci. Instrum.* **67**, 4150–4153.

Meyer-Ilse, W., Medecki, H., Brown, J.T., Heck, J.M., Anderson, E.H., Stead, A., Ford, T., Balhorn, R., Petersen, C., Magowan, C. & Attwood, D.T. (1998) X-Ray microscopy in Berkeley. *X-Ray Microscopy and Spectromicroscopy* (ed. by J. Thieme, G. Schmahl, E. Umbach & D. Rudolph), pp. I1–I12, Springer-Verlag, Heidelberg.

Michette, A.G., Pfauntsch, S.J., Powell, A.K., Graf, T., Losinski, D., McFaul, C.D., Ma, A., Hirst, G.J. & Shaikh, W. (2003) Progress with the King's College laboratory scanning x-ray microscope. *J. Phys. IV, Proc. (France)*, (ed. by J. Susini, D. Joyeux and F. Polack), pp. 123–126, EDP Sciences, Grenoble, France.

Nakayama, S., Haramura, K., Zeng, G.M., Daido, H., Nakatsuka, M., Nakai, S., Katakura, N., Nagata, H. & Aritome, H. (1994) Zone-plate X-ray microscope using a laser-plasma source. *Japan J. Appl. Phys. Part 2-Lett.* **33**, L1280–L1282.

Niemann, B., Rudolph, D. & Schmahl, G. (1976) X-ray microscopy with synchrotron radiation. *Appl. Opt.* **15**, 1883–1884.

Rarback, H., Kenny, J., Kirz, J. & Xie, X. (1980) Scanning X-ray Microscopy-First Tests with Synchrotron Radiation. *Scanned Image Microscopy* (ed. by E. A. Ash), pp. 449–456. Academic Press, London.

Rehbein, S., Holmberg, A., Johansson, G.A., Jansson, P.A.C. & Hertz, H.M. (2004) Fabrication and characterization of a condenser zone plate for compact x-ray microscopy. *J. Vac. Sci. Technol. B* **22**, 1118–1122.

Rudolph, D., Schmahl, G., Niemann, B., Diehl, M., Thieme, J., Wilhein, T., David, C. & Michelman, K. (1994) Wet specimen imaging with an x-ray microscope with a pulsed plasma source. *X-Ray Microscopy IV* (ed. by V.V. Aristov & A.I. Erko), pp. 381–386, Bogorodskii Pechatnik Publishers, Chernogolovka, Moscow, Russia.

Rymell, L. & Hertz, H.M. (1993) Droplet target for low-debris laser-plasma soft-X-ray generation. *Opt. Commun.* **103**, 105–110.

Rymell, L. & Hertz, H.M. (1995) Debris elimination in a droplet-target laser-plasma soft X-ray source. *Rev. Sci. Instrum.* **66**, 4916–4920.

Schmahl, G., Rudolph, D., Niemann, B. & Christ, O. (1980) Zone-plate X-ray microscopy. *Qtr. Rev. Biophys.* **13**, 297–315.

Schmahl, G., Rudolph, D., Niemann, B., Guttmann, P., Thieme, J., Schneider, G., David, C., Diehl, M. & Wilhein, T. (1993) X-ray microscopy studies. *Optik* **93**, 95–102.

Stollberg, H., Guttmann, P., Takman, P.A.C. & Hertz, H.M. (2007) Size-selective colloidal-gold localization in transmission x-ray microscopy. *J. Micros.* **225**, 80–87.

Stollberg, H., Yulin, S., Takman, P.A.C. & Hertz, H.M. (2006) High-reflectivity Cr/Sc multilayer condenser for compact x-ray microscopy. *Rev. Sci. Instrum.* **77**, 123101–1–6.

Vogt, U., Stiel, H., Will, I., Nickles, P.V., Sandner, W., Wieland, M. & Wilhein, T. (2001) Influence of laser intensity and pulse duration on the extreme ultraviolet yield from a water jet target laser plasma. *Appl. Phys. Lett.* **79**, 2336–2338.

von Hofsten, O. (2006), "*Simulation of partially coherent image formation in a compact soft x-ray microscope*." M.Sc. Thesis, Biomedical and X-Ray Physics, Royal Institute of Technology, Sweden.

